

# AGARD

ADVISORY GROUP FOR AEROSPACE RESEARCH & DEVELOPMENT  
7 RUE ANCELLE, 92200 NEUILLY-SUR-SEINE, FRANCE

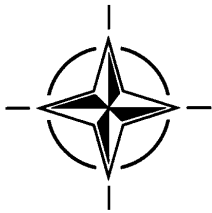
---

**AGARD CONFERENCE PROCEEDINGS 551**

## **Application of Direct and Large Eddy Simulation to Transition and Turbulence**

(L'application de la simulation directe et de la simulation des  
gros tourbillons à la transition et à la turbulence)

*Papers presented and discussions recorded at the 74th Fluid Dynamics Symposium held at  
Chania, Crete, Greece, in April 1994.*



**NORTH ATLANTIC TREATY ORGANIZATION**

---

Published December 1994

*Distribution and Availability on Back Cover*

## THE ASYMPTOTIC STATE OF ROTATING HOMOGENEOUS TURBULENCE AT HIGH REYNOLDS NUMBERS

Kyle D. Squires\*, Jeffrey R. Chasnov†,  
Nagi N. Mansour‡ & Claude Cambon§

Center for Turbulence Research  
Stanford University  
Stanford, CA 94305, USA

### ABSTRACT

The long-time, asymptotic state of rotating homogeneous turbulence at high Reynolds numbers has been examined using large-eddy simulation of the incompressible Navier-Stokes equations. The simulations were carried out using  $128 \times 128 \times 512$  collocation points in a computational domain that is four times longer along the rotation axis than in the other directions. Subgrid-scale motions in the simulations were parameterized using a spectral eddy viscosity modified for system rotation. Simulation results show that in the asymptotic state the turbulence kinetic energy undergoes a power-law decay with an exponent which is independent of rotation rate, depending only on the low-wavenumber form of the initial energy spectrum. Integral lengthscale growth in the simulations is also characterized by power-law growth; the correlation length of transverse velocities exhibiting much more rapid growth than observed in non-rotating turbulence.

### INTRODUCTION AND BACKGROUND

Study of turbulent flows in rotating reference frames has long been an area of considerable scientific and engineering interest. Because of its importance, the subject of turbulence in rotating reference frames has motivated over the years a large number of theoretical, experimental, and computational studies. The bulk of these studies have served to demonstrate that the effect of system rotation on turbulence is subtle and remains exceedingly difficult to predict. For example, it is well recognized that the standard models for the dissipation rate of the turbulent kinetic energy do not accurately predict the effects of system rotation. Yet, these models are widely used in engineering predictive schemes for technologically important areas such as turbomachinery and rotorcraft

aerodynamics.

A rotating flow of particular interest in many studies, including the present work, is examination of the effect of steady system rotation on the evolution of an initially isotropic turbulent flow. Aside from the simplifications associated with analysis and computation of homogeneous flows, one of the principal reasons for the interest in this problem is that solid-body rotation of initially isotropic turbulence represents the most basic turbulent flow whose structure is altered by system rotation but without the complicating effects introduced by mean strains or flow inhomogeneities.

For initially isotropic turbulence it is well known that solid-body rotation inhibits the non-linear cascade of energy from large to small scales. Consequently, the turbulence dissipation rate is reduced relative to non-rotating flows and there is an associated decrease in the decay rate of turbulence kinetic energy [1], [2], [3], [4]. Some computations and experiments have also noted an increase in the integral lengthscales along the rotation axis relative to non-rotating turbulence [5], [6], [7], [8]. Increase in the integral lengthscales has been thought by some to be a prelude to a Taylor-Proudman reorganization to two-dimensional turbulence. However, direct numerical simulation (DNS) has demonstrated that, for very rapid rates of rotation, initially isotropic turbulence remains isotropic and three dimensional [3]. The results in Ref. [3] confirm the essential role of nonlinear interactions for the transition towards two-dimensional turbulence to occur; such a transition, first studied using a spectral approach, can be started only for intermediate Rossby numbers at sufficiently large Reynolds numbers [6], [9].

While some of the effects summarized above are reasonably well documented, e.g., reduction in the decay rate of turbulence kinetic energy, other features of rotating flows are less well resolved, e.g., the behavior of the integral scales. There are also other fundamentally important questions associated with rotating turbulence which cannot be resolved from previous investigations. For example, while the decrease

\*University of Vermont, Burlington, VT, USA

†The Hong Kong University of Science and Technology, Clear Water Bay, Hong Kong

‡NASA Ames Research Center, Moffett Field, CA, USA

§Ecole Centrale de Lyon, Ecully Cedex, France

in the kinetic energy power-law exponent relative to non-rotating turbulence is clear, the actual value is unknown (nor even its dependence on the rotation rate). It is not possible to determine, based upon previous work, whether the effects of rotation on initially isotropic turbulence are transient in nature or an inherent property of rotating flows. Such issues can only be resolved through an examination of the asymptotic state of rotating turbulence; i.e., its long-time evolution. Recent large-eddy simulations of (non-rotating) high Reynolds number isotropic turbulence have demonstrated the universal nature of the flow at long evolution times, including the existence of asymptotic similarity states [10]. It is extension of the ideas in Ref. [10] to rotating turbulence which has been the primary interest of the present work. Knowledge of the asymptotic state of rotating homogeneous turbulence at high Reynolds numbers is further motivated since it will also determine the asymptotic state that engineering turbulence models should yield.

Therefore, the objective of this work has been to examine the long-time evolution of rotating homogeneous turbulence. Of particular interest is the quantification of the asymptotic state at high Reynolds numbers. Important issues in this regard include determining whether the turbulence kinetic energy and integral lengthscales evolve as power laws and, if so, the appropriate exponents for rotating flows. While the power-law decay of the kinetic energy in non-rotating isotropic turbulence is widely accepted, the asymptotic decay of kinetic energy in rotating turbulence is unknown. The behavior of the integral lengthscales at long times in the evolution of rotating flows is also not clear. As discussed above, some previous work suggests an increased growth rate of the integral scales along the rotation axis relative to non-rotating isotropic turbulence. As with the kinetic energy decay, however, it is not clear if this is an effect inherent to rotating flows. Asymptotic power-law behavior of the kinetic energy and integral scales imply the possible existence of similarity states, analogous to those found in the non-rotating flow [10]. Existence of asymptotic similarity states would be of considerable interest since it would permit prediction of the statistical evolution of rotating flows at high Reynolds numbers without requiring knowledge of the complex, and not well understood, non-linear transfer processes.

Large-eddy simulation (LES) is ideally suited for examination of the long-time evolution of rotating homogeneous turbulence. Unlike direct numerical simulation, LES is not restricted to low Reynolds numbers. Aside from the Reynolds number restriction, DNS is further limited to the initial evolution of rotating flows. The need for high Reynolds numbers and long time integrations, as can be obtained using LES, is further motivated by previous studies [3], [6], [9], [10]. The principal drawback to the use of LES is that it requires use of a model to parameterize subgrid-scale stresses. However, in a decaying homogeneous turbulence, the dominant non-linear transfer is from large to small scales so that large-scale statistics may not be unduly influenced by the errors in a

small-scale subgrid model.

The governing equations and an overview of the simulations are provided in the following section. Results from the simulations are then discussed and a summary of the work is contained in the final section.

## SIMULATION OVERVIEW

In the present study the filtered Navier-Stokes equations for an incompressible fluid were solved in a rotating reference frame:

$$\nabla \cdot \mathbf{u} = 0 \quad (1)$$

$$\begin{aligned} \frac{\partial \mathbf{u}}{\partial t} + \mathbf{u} \cdot \nabla \mathbf{u} = & -\frac{1}{\rho} \nabla p - \nabla \cdot \boldsymbol{\tau} \\ & + \nu \nabla^2 \mathbf{u} - 2\boldsymbol{\Omega} \times \mathbf{u}. \end{aligned} \quad (2)$$

In (1) and (2),  $\mathbf{u}$  is the (filtered) velocity vector,  $p$  and  $\rho$  the fluid pressure and density, respectively, and  $\nu$  the kinematic viscosity. The Coriolis term in (2) accounts for reference frame rotation, the rotation vector is denoted  $\boldsymbol{\Omega}$  and, for the purposes of discussion, is considered to act along the  $z$  or "vertical" axis,  $\boldsymbol{\Omega} = (0, 0, \Omega)$ . Filtering of the convective terms yields the subgrid-scale stress  $\boldsymbol{\tau}$  in (2) and this term requires a model in order to represent the effect of subgrid-scale motions on the resolved scales.

In this work the subgrid-scale stresses have been parameterized in the Fourier space using a spectral eddy viscosity which accounts for system rotation. The form of the eddy viscosity for non-rotating turbulence is [11]:

$$\begin{aligned} \nu_e(k|k_m, t) = & \left[ 0.145 + 5.01 \exp\left(\frac{-3.03k_m}{k}\right) \right] \\ & \times \left[ \frac{E(k_m, t)}{k_m} \right]^{1/2} \end{aligned} \quad (3)$$

where  $\nu_e$  is the eddy viscosity,  $k_m$  the maximum wavenumber magnitude of the simulation and  $E(k, t)$  is the spherically integrated three-dimensional Fourier transform of the co-variance  $\frac{1}{2} \langle u_i(\mathbf{x}, t) u_i(\mathbf{x} + \mathbf{r}, t) \rangle$  ( $\langle \cdot \rangle$  denotes a volume average). In this work the eddy viscosity  $\nu_e$  has been modified to account for the weakening of the energy cascade in a rotating turbulence:

$$\nu_\Omega = \nu_e f(\alpha). \quad (4)$$

In (4),  $\nu_\Omega$  is the eddy viscosity in rotating turbulence with the function  $f(\alpha)$  accounting for the reduction by system rotation. Using an EDQNM model modified to take into account the effect of rotation on the energy cascade [12], it is possible to calculate the factor  $f(\alpha)$  (see Ref. [13], later corrected by [14]):

$$f(\alpha) = \frac{2[(1 + \alpha^2)^{3/2} - \alpha^3 - 1]}{3\alpha^2} \quad (5)$$

where

$$\alpha = \frac{8\Omega^2}{3E(k_m)k_m^3}. \quad (6)$$

As can be seen from (5) and (6), the eddy viscosity is reduced for increasing  $\Omega$ . It is also worth noting that (4)–(6) yields an expression similar in form to the reduction in velocity derivative skewness by rotation found in Ref. [3] using DNS of rotating isotropic turbulence. Some comparisons between different sub-grid models (including a dynamic model [4]) and the one used in this study (4), (5), and (6) are reported in [15].

The initial energy spectrum of the simulations was of the form

$$E(k, 0) = \frac{1}{2} C_s \frac{u_0^2}{k_p} \left( \frac{k}{k_p} \right)^s \exp \left[ -\frac{1}{2} s \left( \frac{k}{k_p} \right)^2 \right], \quad (7)$$

where  $C_s$  is given by

$$C_s = \sqrt{\frac{2}{\pi}} \frac{s^{\frac{1}{2}(s+1)}}{1 \cdot 3 \cdot \dots \cdot (s-1)} \quad (8)$$

and  $k_p$  is the wavenumber at which the initial energy spectrum is maximum. In this study simulations with  $s = 2$  and  $s = 4$  were performed, corresponding to the initial energy spectrum having a low wavenumber form proportional to either  $k^2$  or  $k^4$ .

Because the principal interest of this work was examination of the long-time evolution of rotating homogeneous turbulence, it was necessary to use as large a value of  $k_p$  as possible in order that the flow evolution not be adversely affected by the periodic boundary conditions used in the simulations. Adverse effects occur when the integral lengthscales of the flow become comparable to the box size. Another important consideration in these simulations was the aspect ratio of the computational domain. Because of the rapid growth of the integral scales along the direction of the rotation axis, it was necessary to use a computational box which was longer along the rotation axis than in the other directions. Preliminary calculations of rotating turbulence on cubic domains demonstrated a relatively rapid degradation in the integral scales in the vertical direction because of periodic boundary conditions. Numerical experiments showed that it was optimal to use a computational box which was four times longer along the rotation axis than in the directions orthogonal to the rotation vector. Four times as many collocation points were used in the vertical direction in order to avoid any effects of grid anisotropy at the smallest resolved scales.

Simulations were performed using resolutions of  $128 \times 128 \times 512$  collocation points. The governing equations (1) and (2) were solved using a pseudo-spectral method [16]. The length of the computational box along the vertical axis was  $\sqrt[3]{128\pi}$ , corresponding to a minimum wavenumber of 0.397 and maximum of 95. The lengths of the computational volume in the horizontal plane (orthogonal to the rotation axis) were  $\sqrt[3]{2\pi}$ , corresponding to a minimum wavenumber of 1.587 and maximum of 95. The initial root-mean-square velocity fluctuation  $u_0$  in (7) was equal to 1/2 and the wavenumber at which

the initial spectrum was initially maximum,  $k_p$ , was 75. The initial energy spectrum was set to zero for wavenumbers greater than 93 to allow the sub-grid-scale eddy viscosity to build up from zero values. For each spectrum type, i.e., low wavenumber part proportional to  $k^2$  or  $k^4$ , simulations were performed with  $\Omega = 0, 0.5$ , and 1.0.

Finally, it is also noted that statistics from simulations performed on a domain having resolutions of  $96 \times 96 \times 384$  collocation points were in good agreement with the results presented in this paper. The principal advantage of the higher resolution simulations is the increase in time the flow field maintains its asymptotic state before the simulation results are impacted by the finite computational domain.

## RESULTS

The time development of the resolved-scale turbulence kinetic energy,  $\langle \mathbf{u}^2 \rangle$ , for both initial spectrum types is shown in Figure 1 for each rotation rate. The time axis in Figure 1 and following figures has been made dimensionless using the eddy turnover time in the initial field

$$\tau(0) = L_u(0) / \langle \mathbf{u}^2 \rangle \quad (9)$$

where  $L_u(t)$  is the velocity integral scale at time  $t$  defined as

$$L_u(t) = \frac{\pi}{2} \frac{\int_0^\infty k^{-1} E(k, t) dk}{\int_0^\infty E(k, t) dk}. \quad (10)$$

In isotropic turbulence,  $L_u$  is two-thirds the usual longitudinal integral scale measured in experiments. Throughout this work, “ $k^2$  spectrum” refers to an initial energy spectrum  $E(k)$  with low wavenumber part proportional to  $k^2$  while “ $k^4$  spectrum” refers to an initial  $E(k)$  with low wavenumbers proportional to  $k^4$ . The characteristic effect of increasing  $\Omega$  on the evolution of  $\langle \mathbf{u}^2 \rangle$  is evident in Figure 1, i.e., inhibition of the energy cascade with increasing rotation rate resulting in a less rapid decay of kinetic energy.

The effect of rotation on the evolution of turbulence kinetic energy is even more clearly seen in Figure 2. Plotted in Figure 2 is the power-law exponent of  $\langle \mathbf{u}^2 \rangle$  for each rotation rate and initial spectrum type. It is evident from Figure 2 that, following an initial transient, the power-law exponent becomes independent of time.

The values of the power-law exponents for the simulations at zero rotation rate are in good agreement with the simulations of Ref. [10] despite the anisotropic computational box. Comparison of the power-law exponents for a given initial spectrum type clearly show the reduction in the decay rate of kinetic energy in rotating turbulence. It may be observed that for both initial spectrum types, the power-law exponent is reduced by approximately a factor of two in rotating turbulence relative to its value at  $\Omega = 0$ . Finally, in the asymptotic region the

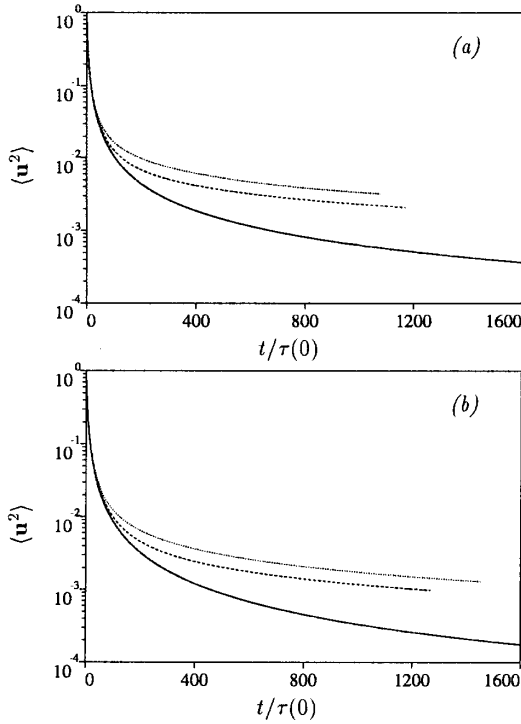


Figure 1: Time development of resolved-scale kinetic energy in rotating turbulence. —,  $\Omega = 0$ ; ----,  $\Omega = 0.5$ ; ·····,  $\Omega = 1.0$ . (a)  $k^2$  spectrum; (b)  $k^4$  spectrum.

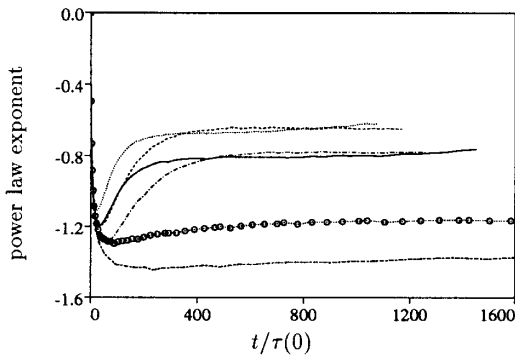


Figure 2: Time development of the power-law exponent of  $\langle \mathbf{u}^2 \rangle$  in rotating turbulence.  $k^2$  spectrum:  $\circ \cdots \circ$ ,  $\Omega = 0$ ; ----,  $\Omega = 0.5$ ; ·····,  $\Omega = 1.0$ .  $k^4$  spectrum: —,  $\Omega = 0$ ; — — —,  $\Omega = 0.5$ ; — — — —,  $\Omega = 1.0$ .

power-law exponent of  $\langle \mathbf{u}^2 \rangle$  is independent of the rotation rate, depending only on the form of the initial energy spectrum.

Chasnov [10] showed that, at high Reynolds numbers, the asymptotic decay of  $\langle \mathbf{u}^2 \rangle$  in isotropic turbulence could be accurately described using simple scaling arguments and dimensional analysis. The analysis is predicated on the assumption that the asymptotic scaling of  $\langle \mathbf{u}^2 \rangle$  is dependent on the form of  $E(k)$  at low wavenumbers and independent of viscosity. For high Reynolds number turbulence this is reasonable since the direct effect of viscosity occurs at much higher wavenumber magnitudes than those scales which contain most of the energy. The asymptotic forms found in [10] can be obtained by first considering an asymptotic series expansion of the energy spectrum near  $k = 0$

$$E(k) = 2\pi k^2 (B_0 + B_2 k^2 + \dots). \quad (11)$$

The initial  $E(k)$  with low wavenumbers proportional to  $k^2$  corresponds to a non-zero value of  $B_0$  while the  $k^4$  spectrum is obtained for  $B_0 = 0$  and non-zero  $B_2$ . Saffman [17] considered a homogeneous turbulence field generated by a distribution of random impulsive forces and showed that as a consequence of momentum conservation  $B_0$  is invariant in time. Batchelor & Proudman [18] considered an initial flow field in which all of the velocity cumulants of the turbulence are exponentially small at large separations distances. For this flow  $B_2$  (the Loitsianski integral) is non-zero but not time invariant. Closure calculations [19] and large-eddy simulations [20] have shown that the time dependence of  $B_2$  is weak relative to the overall turbulence decay, however, and is therefore assumed constant for the sake of obtaining an approximate asymptotic scaling law for  $\langle \mathbf{u}^2 \rangle$ . Thus, assuming the appropriate dependence of  $\langle \mathbf{u}^2 \rangle$  on either  $B_0$  or  $B_2$ , dimensional analysis yields the asymptotic scaling of  $\langle \mathbf{u}^2 \rangle$  for non-rotating turbulence [10]

$$\langle \mathbf{u}^2 \rangle \propto B_0^{2/5} t^{-6/5} \quad (k^2 \text{ spectrum}) \quad (12)$$

and

$$\langle \mathbf{u}^2 \rangle \propto B_2^{2/7} t^{-10/7} \quad (k^4 \text{ spectrum}). \quad (13)$$

as previously obtained by Saffman [21] and Kolmogorov [22].

The results above may be generalized for rotating homogeneous turbulence by considering the additional dimensionless group for this flow,  $\Omega t$ . For the rotating flow a dimensional analysis yields the following possible asymptotic decay:

$$\langle \mathbf{u}^2 \rangle \propto B_0^{2/5} t^{-6/5} (\Omega t)^x \quad (k^2 \text{ spectrum}) \quad (14)$$

$$\langle \mathbf{u}^2 \rangle \propto B_2^{2/7} t^{-10/7} (\Omega t)^{x'} \quad (k^4 \text{ spectrum}). \quad (15)$$

For rotating turbulence at high Reynolds numbers and low Rossby numbers it is possible to offer plausibility arguments to determine the unknown exponents  $x$  and  $x'$ . In this regime rotating turbulence is characterized by two disparate timescales, a long

timescale representative of the turbulence evolution and a short timescale associated with the rotation frequency,  $\Omega$ . If it is assumed that the correlation time of the non-linear triadic interactions is directly proportional to the short timescale  $1/\Omega$ , then the transport equation of  $\langle \mathbf{u}^2 \rangle$  may be written as

$$\frac{d\langle \mathbf{u}^2 \rangle}{dt} = \frac{1}{\Omega} f(T, B_0 \text{ or } B_2) \quad (16)$$

for the two initial spectrum types. The long timescale of the non-linear interactions in (16) is denoted  $T$  and may be constructed on dimensional grounds from  $\langle \mathbf{u}^2 \rangle$  and  $B_0$  or  $B_2$ . Dimensional analysis may be used to determine the unknown function  $f$ , yielding

$$\frac{d\langle \mathbf{u}^2 \rangle}{dt} = \frac{1}{\Omega} B_0^{-2/3} \langle \mathbf{u}^2 \rangle^{8/3} \quad (17)$$

for non-zero  $B_0$  and

$$\frac{d\langle \mathbf{u}^2 \rangle}{dt} = \frac{1}{\Omega} B_2^{-2/5} \langle \mathbf{u}^2 \rangle^{12/5} \quad (18)$$

for zero  $B_0$ . Integrating (17) and (18) results in the predicted asymptotic decay for  $\langle \mathbf{u}^2 \rangle$  in rotating turbulence:

$$\langle \mathbf{u}^2 \rangle \propto B_0^{2/5} \Omega^{3/5} t^{-3/5} \quad (k^2 \text{ spectrum}) \quad (19)$$

and

$$\langle \mathbf{u}^2 \rangle \propto B_2^{2/7} \Omega^{5/7} t^{-5/7} \quad (k^4 \text{ spectrum}). \quad (20)$$

The scaling laws (19) and (20) predict that in rotating turbulence the kinetic energy decay exponent is reduced by a factor of two relative to its value in the non-rotating flow (cf. 14 and 15). More importantly, the exponents predicted from (19) and (20) and the actual values obtained in the simulations (Figure 2) are in very good agreement. The actual value of the power-law exponent for cases with non-zero  $B_0$  is around -0.65, compared to a predicted value of -0.6, while the exponent in the asymptotic region for simulations with zero  $B_0$  is approximately -0.78, slightly smaller than the predicted value of -0.71. Thus, neglecting the weak time dependence of the leading order term  $B_2$ , necessary in order to obtain (20), appears justified.

While the asymptotic scaling laws (19) and (20) yield exponents for the dependence of  $\langle \mathbf{u}^2 \rangle$  on time which are in good agreement with the large-eddy simulations, it is not possible to verify the power-law dependence of the kinetic energy on  $\Omega$  using the results in Figure 2. To test the scaling of  $\langle \mathbf{u}^2 \rangle$  on  $\Omega$ , the quantities

$$\frac{\langle \mathbf{u}^2 \rangle}{B_0^{2/5} \Omega^{3/5} t^{-3/5}} \quad (21)$$

and

$$\frac{\langle \mathbf{u}^2 \rangle}{B_2^{2/7} \Omega^{5/7} t^{-5/7}} \quad (22)$$

are plotted in Figure 3. Note that the value of  $B_2$  used in (22) is from the initial condition. Provided that the dependence on  $\Omega$  shown in (19) and (20) is

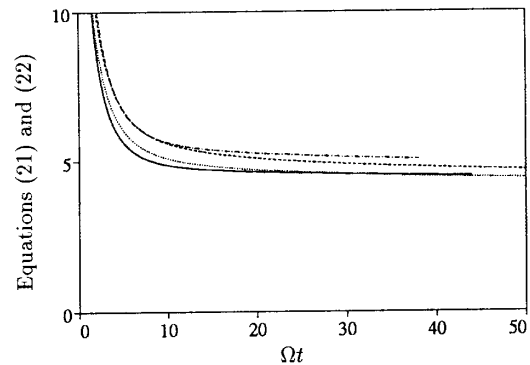


Figure 3: Check of asymptotic scaling laws (19) and (20).  $k^2$  spectrum: —,  $\Omega = 0.5$ ; ·····,  $\Omega = 1.0$ .  $k^4$  spectrum: — —,  $\Omega = 0.5$ ; - - - -,  $\Omega = 1.0$ .

correct, (21) and (22) in Figure 3 should asymptote to the same dimensionless constant at long times (for a given initial spectrum type). The results in Figure 3 show that the collapse of the kinetic energy obtained using the asymptotic scaling laws is excellent for the  $k^2$  spectrum. For the  $k^4$  spectrum the collapse is reasonable considering the assumption of a time-invariant  $B_2$ . It may be concluded that Figure 3 validates the scalings on rotation rate as obtained from the analysis leading to (19) and (20).

In rotating turbulence it is possible that the velocity fluctuations along the rotation axis may possess a different power-law decay than those in the plane normal to the rotation vector (i.e., the horizontal plane). It is not clear based upon previous numerical and experimental results as to the behavior of the vertical fluctuations  $\langle w^2 \rangle$  relative to the velocity scale in the horizontal plane,  $(\langle u^2 \rangle + \langle v^2 \rangle)/2$ . Shown in Figure 4 is the ratio of  $(\langle u^2 \rangle + \langle v^2 \rangle)/2$  to the vertical fluctuations,  $\langle w^2 \rangle$ . With the exception of the highest rotation rate in the simulations with non-zero  $B_0$ , the results in Figure 4 show that in the asymptotic region the ratio of mean-square velocity fluctuations is approximately 0.8. This result is further significant since it also implies the existence in the asymptotic region of a single velocity scale in rotating turbulence.

For the rotating flow, by axisymmetry, there are possibly five independent lengthscales. These integral scales are obtained from integration of the two-point correlation function

$$L_{\alpha\alpha;\beta} = \frac{1}{\langle u_\alpha^2 \rangle} \int \langle u_\alpha(\mathbf{x}) u_\alpha(\mathbf{x} + r_\beta) \rangle dr_\beta. \quad (23)$$

The lengthscale  $L_{\alpha\alpha;\beta}$  measures the correlation between the  $\alpha$  velocity components with separation in the  $\beta$  direction. In the horizontal plane the independent lengthscales may be expressed using (23) as

$$\begin{aligned} L_{h1} &= (L_{11,1} + L_{22,2})/2 \\ L_{h2} &= (L_{11,2} + L_{22,1})/2 \\ L_{h3} &= (L_{33,1} + L_{33,2})/2. \end{aligned} \quad (24)$$

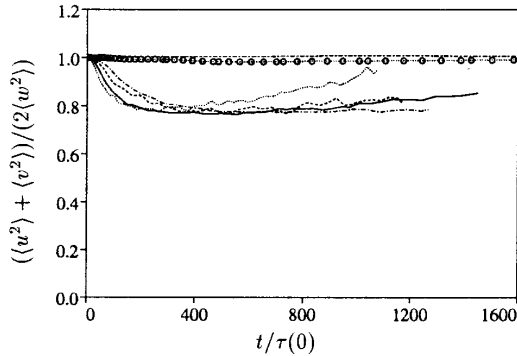


Figure 4: Time development of mean-square velocity ratio in rotating turbulence.  $k^2$  spectrum:  $\circ \cdots \circ$ ,  $\Omega = 0$ ;  $-\cdots-$ ,  $\Omega = 0.5$ ;  $\cdots \cdots$ ,  $\Omega = 1.0$ .  $k^4$  spectrum:  $-\cdots-$ ,  $\Omega = 0$ ;  $-\cdots-$ ,  $\Omega = 0.5$ ;  $-\cdots-$ ,  $\Omega = 1.0$ .

The integral scale  $L_{h1}$  measures the horizontal correlation of longitudinal velocities,  $L_{h2}$  the horizontal correlation of lateral velocities, and  $L_{h3}$  the correlation in the horizontal plane of vertical velocity fluctuations. For the vertical direction (along the rotation axis) the two independent integral scales are

$$\begin{aligned} L_{v1} &= (L_{11,3} + L_{22,3})/2 \\ L_{v2} &= L_{33,3} \end{aligned} \quad (25)$$

where  $L_{v1}$  measures the vertical correlation of lateral velocities and  $L_{v2}$  the vertical correlation of vertical velocities.

For the non-rotating flow dimensional analysis yields directly the asymptotic scalings of the integral scales for high Reynolds number isotropic turbulence [10]

$$L_u \propto B_0^{1/5} t^{2/5} \quad (k^2 \text{ spectrum}) \quad (26)$$

$$L_u \propto B_2^{1/7} t^{2/7} \quad (k^4 \text{ spectrum}). \quad (27)$$

For the rotating flow the appropriate dependence of the integral scales on the invariant  $B_0$  and approximate invariant  $B_2$  can be approached in the same manner as for the kinetic energy, i.e., through introduction of the additional dimensionless group  $\Omega t$  with appropriate exponents. For example, for the vertical lengthscales  $L_{v2}$  the development in the asymptotic state may be expressed as

$$L_{v2} \propto B_0^{1/5} t^{2/5} (\Omega t)^{y_2} \quad (k^2 \text{ spectrum}) \quad (28)$$

and

$$L_{v2} \propto B_2^{1/7} t^{2/7} (\Omega t)^{y_2'} \quad (k^4 \text{ spectrum}). \quad (29)$$

Using (24) and (25) one could write similar expressions for the other lengthscales; each with a possibly distinct exponent as in (28) and (29). Unlike the kinetic energy, however, we do not yet have an argument for predicting *a priori* the appropriate exponents for the integral lengthscale growth in the rotating flow. Rather, the results of the large-eddy

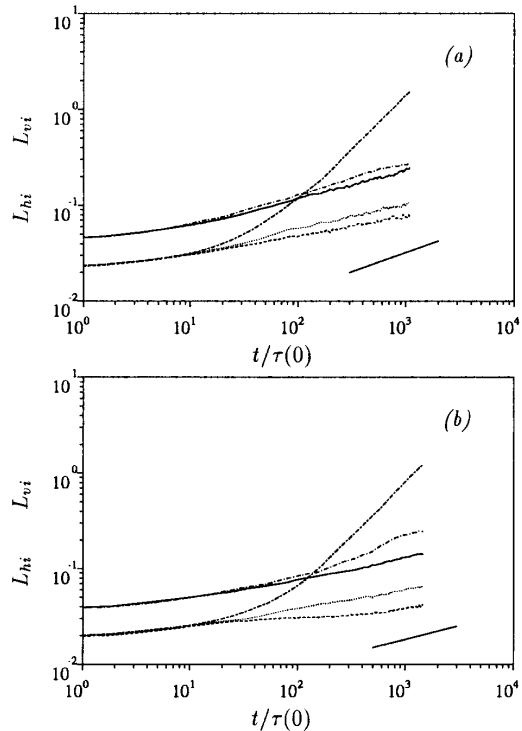


Figure 5: Time development of integral lengthscales in rotating turbulence,  $\Omega = 1$ . Asymptotic growth rate in non-rotating turbulence also shown in lower portion of Figure.  $-\cdots-$ ,  $L_{h1}$ ;  $-\cdots-$ ,  $L_{h2}$ ;  $\cdots \cdots$ ,  $L_{h3}$ ;  $-\cdots-$ ,  $L_{v1}$ ;  $-\cdots-$ ,  $L_{v2}$ . (a)  $k^2$  spectrum; (b)  $k^4$  spectrum.

simulations are used to supply the unknown exponents.

Shown in Figure 5 is the time development of the integral scales for both initial spectrum types. The curves shown in Figure 5 are for the highest rotation rate used with each initial condition. Also shown for reference in both Figures is the slope corresponding to the asymptotic growth rate in non-rotating isotropic turbulence. It is clear from Figure 5 that the growth of  $L_{v1}$  is much more rapid than the asymptotic growth rate in non-rotating turbulence as well as the other integral scales in the rotating flow. With the exception of  $L_{v1}$ , the growth rate of the integral scales in the rotating flow are slightly suppressed relative to the non-rotating case. More importantly, the simulation results demonstrate that in the asymptotic region the integral lengthscales do in fact exhibit power-law growth and, with the exception of  $L_{v1}$ , the power-law exponents of the integral scales are identical. Thus, in the horizontal plane there is a single independent lengthscale,  $L_h$ , while there exist two independent integral scales in the vertical,  $L_{v1}$  and  $L_{v2}$ . The asymptotic scaling laws obtained from the simulations for the  $k^2$  spectrum are approximately

$$\begin{aligned} L_h &\propto B_0^{1/5} \Omega^{-3/20} t^{1/4} \\ L_{v1} &\propto B_0^{1/5} \Omega^{3/5} t^1 \\ L_{v2} &\propto B_0^{1/5} \Omega^{-3/20} t^{1/4} \end{aligned} \quad (30)$$

while for the  $k^4$  spectrum the long-time evolution of the lengthscales determined from the large-eddy simulations are approximately

$$\begin{aligned} L_h &\propto B_2^{1/7} \Omega^{-3/35} t^{1/5} \\ L_{v1} &\propto B_2^{1/7} \Omega^{32/35} t^{6/5} \\ L_{v2} &\propto B_2^{1/7} \Omega^{-3/35} t^{1/5} \end{aligned} \quad (31)$$

Perhaps the most striking feature of the integral scale behavior is that even in the asymptotic region the growth of  $L_{v1}$  is much more rapid than the other lengthscales. Surprisingly, the vertical correlation of vertical velocities,  $L_{v2}$ , is relatively unaffected by rotation which would seem to indicate a “de-coupling” between the two vertical lengthscales. However, this de-coupling occurs while there is close coupling between  $L_h$  and  $L_{v2}$  as well as between the velocity components in the vertical and horizontal planes (Figure 4).

The relations (30) and (31) yield the appropriate dependence of the integral lengthscales on time but, similar to the kinetic energy considered earlier, it is not possible to verify the dependence on rotation rate from the results in Figure 5. Shown in Figure 6 are the ratio of the integral lengthscales to the appropriate combination of  $B_0$ ,  $B_2$ ,  $\Omega$ , and  $t$ , i.e.,

$$\begin{aligned} L_h, L_{v2} &/ \left( B_0^{1/5} \Omega^{-3/20} t^{1/4} \right) \\ L_{v1} &/ \left( B_0^{1/5} \Omega^{3/5} t^1 \right) \end{aligned} \quad (32)$$

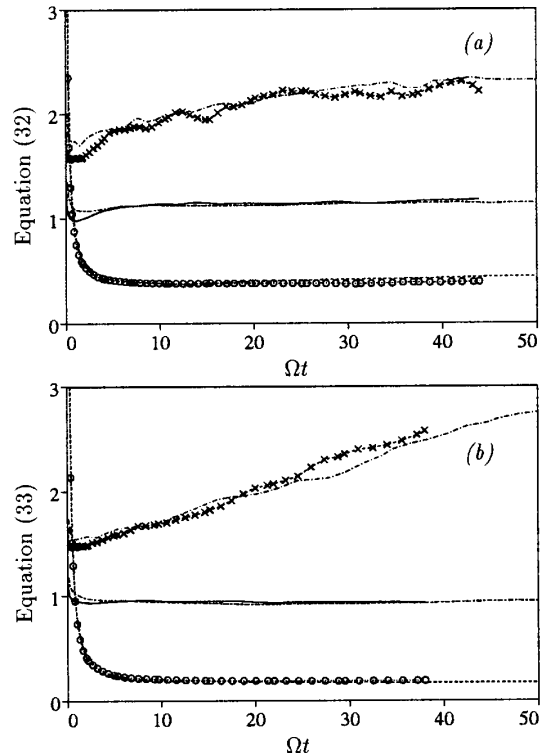


Figure 6: Check of asymptotic scaling laws (30) and (31).  $\Omega = 0.5$ : —,  $L_h$ ;  $\circ \cdots \circ$ ,  $L_{v1}$ ;  $\times \cdots \times$ ,  $L_{v2}$ .  $\Omega = 1.0$ : - - -,  $L_h$ ; - - - -,  $L_{v1}$ ; - - - -,  $L_{v2}$ . (a)  $k^2$  spectrum; (b)  $k^4$  spectrum.

for the  $k^2$  spectrum (Figure 6a) and

$$\begin{aligned} L_h, L_{v2} &/ \left( B_2^{1/7} \Omega^{-3/35} t^{1/5} \right) \\ L_{v1} &/ \left( B_2^{1/7} \Omega^{32/35} t^{6/5} \right) \end{aligned} \quad (33)$$

for the  $k^4$  spectrum (Figure 6b). The collapse of the lengthscales for the different rotation rates in Figure 6 demonstrates that the scalings (30) and (31) possess the proper dependence on the rotation rate. The collapse of the integral scales  $L_{v1}$  is especially striking given the relatively strong dependence on  $\Omega$ . Figure 6 also demonstrates an excellent collapse of the horizontal integral scale  $L_h$ . The collapse of  $L_{v2}$  using the (30) and (31) for different  $\Omega$  possesses the greatest amount of statistical variation, presumably due to the fewer number of samples available to compute this lengthscale.

## SUMMARY

Large-eddy simulations of high Reynolds number rotating homogeneous turbulence have been performed. The calculations were evolved sufficiently far in time to observe the development of the asymptotic state for initial conditions with low wavenumbers proportional to both  $k^2$  and  $k^4$ . The simula-



tions demonstrate the characteristic effect of solid body rotation on initially isotropic turbulence, i.e., inhibition of non-linear energy transfer from large to small scales and less rapid decay of kinetic energy. In the asymptotic region the decay exponent of the turbulence kinetic energy is also observed to be independent of time as well as rotation rate.

Simple scaling arguments and dimensional analysis were used to obtain predictions of the asymptotic behavior of the kinetic energy. Assuming that the non-linear triadic interactions have a correlation time directly proportional to the rotation time scale allows one to predict *a priori* the asymptotic scaling laws for the turbulence kinetic energy. The predicted values were found to be in very good agreement with the simulation results, supporting the analytical results.

In the rotating flow simulation results indicate that in the asymptotic region the integral lengthscales undergo a power-law growth. With the exception of the correlation length along the rotation axis of horizontal velocities, integral lengthscale growth in the rotating flows is found to be slightly suppressed relative to non-rotating isotropic turbulence. In the asymptotic region there is a single horizontal lengthscale but two independent vertical lengthscales. The de-coupling between the vertical lengthscales was unexpected, especially considering the strong coupling between the vertical and horizontal velocity fluctuations.

More work is required to better understand the asymptotic state of rotating turbulent flows at high Reynolds numbers. Application of the scaling laws to the appropriately defined energy spectra is needed to further validate the similarity states indicated by the power-law evolution in the kinetic energy and integral lengthscales found in this work. Use of the database accumulated during the course of this work will also be invaluable for future studies directed towards extension of engineering turbulence models to high Reynolds number rotating flows.

#### ACKNOWLEDGMENTS

The authors gratefully acknowledge the support of Dr. Robert Rogallo and Dr. Alan Wray at the NASA Ames Research Center. Partial support for this work was obtained from the American Society for Engineering Education. The computations were performed on the Cray C-90 at NASA Ames.

#### REFERENCES

- [1] Traugott, S.C., "Influence of solid-body rotation on screen-produced turbulence", *NACA TN 4135*, 1958.
- [2] Veeravalli, S.V., "An experimental study of the effects of rapid rotation on turbulence", *Annual Research Briefs - 1991*, NASA-Stanford Center for Turbulence Research, 1991.
- [3] Mansour, N.N., Cambon, C. & Speziale, C.G., "Theoretical and computational study of rotating isotropic turbulence", in *Studies in Turbulence*, edited by T. B. Gatski, S. Sarkar & C. G. Speziale, Springer-Verlag, 1992.
- [4] Squires, K.D. & Piomelli, U., "Dynamic modeling of rotating turbulence", in press, *Turbulent Shear Flows 9*, edited by F. Durst, N. Kasagi, B.E. Launder, F.W. Schmidt and J.H. Whitelaw, Springer Verlag, 1994.
- [5] Bardina, J., Ferziger, J.H. & Rogallo, R.S., "Effect of rotation on isotropic turbulence: computation and modeling", *J. Fluid Mech.* **154**, 321, 1985.
- [6] Jacquin, L., Leuchter, O., Cambon, C. & Mathieu, J., "Homogeneous turbulence in the presence of rotation", *J. Fluid Mech.* **220**, 1, 1990.
- [7] Bartello, P., Métais, O. & Lesieur, M., "Coherent structures in rotating three-dimensional turbulence", submitted to *J. Fluid Mech.*
- [8] Hossain, M., "Reduction in the dimensionality of turbulence due to a strong rotation", *Phys. Fluids A* **6**, 1077, 1994.
- [9] Cambon, C. & Jacquin, L., "Spectral approach to non-isotropic turbulence subjected to rotation", *J. Fluid Mech.* **202**, 295, 1989.
- [10] Chasnov, J.R., "Similarity states of passive scalar transport in isotropic turbulence", *Phys. Fluids A* **6**, 1036, 1994.
- [11] Chollet, J.P. & Lesieur, M., "Parameterization of small scales of three-dimensional isotropic turbulence utilizing spectral closures", *J. Atmos. Sci.* **38**, 2747, 1981.
- [12] Cambon C., Bertoglio, J.P. & Jeandel, D., "Spectral closure of homogeneous turbulence", AFOSR-Stanford Conf. on Complex Turb. Flows, 1981.
- [13] Aupoix, B., "Eddy viscosity subgrid-scale models for homogeneous turbulence", in *Proc. of Macroscopic Mod. Turb. Flows, Lecture Notes in Phys.*, **230**, 45, 1984.
- [14] Alexandre A. & Bertoglio, J.P., private communication, 1992.
- [15] Cambon, C., Bertoglio, J.P., Godefert, F.S. & Le Penven, L., in *Report on the 1993 Summer School/Workshop: Modelling Turbulent Flows - ERCOFTAC Bulletin # 19*, 1993.
- [16] Rogallo, R.S., "Numerical experiments in homogeneous turbulence", *NASA TM 81315*, 1981.
- [17] Saffman, P.G., "The large-scale structure of homogeneous turbulence", *J. Fluid Mech.* **27**, 581, 1967.

- [18] Batchelor, G. K. & Proudman, I., "The large-scale structure of homogeneous turbulence", *Phil. Trans. Roy. Soc.*, **248**, 369, 1956.
- [19] Lesieur, M., *Turbulence in Fluids*, Nijhoff, 1990.
- [20] Chasnov, J.R., "Computation of the Loitsian-ski integral in decaying isotropic turbulence", *Phys. Fluids A* **5**, 2579, 1993.
- [21] Saffman, P.G., "Note on decay of homogeneous turbulence", *Phys. Fluids* **10**, 1349, 1967.
- [22] Kolmogorov, A.N., "On degeneration of isotropic turbulence in an incompressible viscous liquid", *Dokl. Akad. Nauk. SSSR*, **31**, 538, 1941.